Title

Optimization of neutron tomography for rapid hydrogen concentration inspection of metal castings

Authors

Gibbons, Matthew R.
Richards, Wade J.
Shields, Kevin

Publication Date

1999-11-03

Peer reviewed

ELSEVIER

Nuclear Instruments and Methods in Physics Research A 424 (1999) 53–57

NUCLEAR INSTRUMENTS & METHODS IN PHYSICS RESEARCH Section A

Optimization of neutron tomography for rapid hydrogen concentration inspection of metal castings

Matthew R. Gibbons, Wade J. Richards*, Kevin Shields

McClellan Nuclear Radiation Center, SM-ALC/TIR, 5335 Price Ave., McClellan AFB, CA 95652,USA

Abstract

Hydrogen embrittlement describes a group of phenomena leading to the degradation of metal alloy properties. The hydrogen concentration in the alloy can be used as an indicator for the onset of embrittlement. A neutron tomography system has been optimized to perform nondestructive detection of hydrogen concentration in titanium aircraft engine compressor blades. Preprocessing of backprojection images and postprocessing of tomographic reconstructions are used to achieve hydrogen concentration sensitivity below 200 ppm weight. This paper emphasizes the postprocessing techniques which allow automated reporting of hydrogen concentration.

PACS: 28.41.Rc; 42.30.Wb; 81.40.Np; 81.70.Yp

Keywords: Neutron computed tomography; Neutron radiography; Hydrogen embrittlement; Nondestructive testing

1. Introduction

This paper describes the neutron tomography system at the McClellan Nuclear Radiation Center (MNRC) with emphasis on the automated procedures for quantitative determination of hydrogen concentrations in metal components. The system was developed as a result of the need to obtain hydrogen concentration data for aircraft engine compressor blades. The hydrogen concentration can be used as an indicator for the loss of mechanical properties, embrittlement, which can occur in metals after exposure to hydrogen [1]. The requirements for the system include the evaluation of large parts (tens of cm) with small features (< 1 cm) at a rate of several per hour. Additionally, hydrogen concentrations must be detected accurately from 200 ppm weight to several thousand ppm.

The tomography system consists of a neutron source, object turntable, scintillator screen, mirror, CCD camera, and computer support [2] and is similar to McFarland et al. [3,4]. The neutron source is a 2 MW research reactor. The neutron beam is approximately 50 cm in diameter at the scintillation screen with a thermal flux of $10^7 \mathrm{n/cm^2\,s}$. The system can acquire 180 images with 0.057 cm resolution in one hour. The

* Corresponding author.

0168-9002/99/$ – see front matter
PII: S0168-9002(98)01297-2

tomographic reconstruction algorithm calculates the spatial distribution of the macroscopic neutron cross section in an object from the attenuation of the neutron beam as it passes through the object at different angles. The hydrogen content has been calibrated against the increase in the macroscopic cross section. Besides reconstruction with the filtered backprojection method [5], preprocessing of backprojection images as well as postprocessing of tomographic reconstructions are used to achieve the required hydrogen concentration sensitivity and spatial resolution.

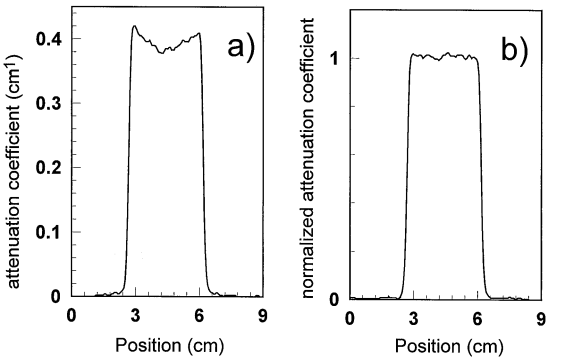

Fig. 1. Cross section of the NIST Ti6Al4V disk reconstruction when (a) backprojection preprocessing was not performed, and (b) preprocesssing was performed.

2. Image preprocessing and hydrogen signal

Before the backprojection images are given to the reconstruction routine, preprocessing is required to ensure that the beam intensity in the images is an accurate representation of the attenuation caused by the objects imaged [6]. The procedures are detailed in a recent article [2], and only a summary will be presented here.

A dark charge image is taken and subtracted automatically during image acquisition. The images are then divided by the unobstructed beam image leaving the normalized attenuated signal. The average flux from the MNRC reactor has some fluctuation with time. The average intensity in an unobstructed part of the beam in each normalized image determines the correction factor for reactor fluctuations. A relatively uniform background noise signal was also measured. This background signal is due to scattered light from the scintillation screen and scattered neutrons from the beam stop and other structures in the radiography bay. The background noise and any object neutron scattering signals are determined from the intensity behind a borated-poly strip which is placed between the object and the beam. This strip is opaque to the neutron beam so any signal behind the strip is subtracted from each image's intensity.

The attenuation coefficient line integral must be calculated for each pixel in the backprojection images. Since the neutron beam not monoenergetic, beam hardening errors are mitigated by using a table of attenuation length versus intensity. The table was generated from measurements of intensity behind titanium alloy standards of known thickness. These standards were obtained from the National Institute of Standards and Technology and were certified to have less than 50 ppm hydrogen. The table provides attenuation lengths normalized to the Ti alloy so samples of the pure alloy should have attenuation coefficients of 1.0 after reconstruction. Measurement of test samples also provided the attenuation coefficient corresponding to particular densities of hydrogen. Over a wide range of concentrations the attenuation coefficient for 100 ppm hydrogen relative to the attenuation coefficient of titanium is 0.02. The preprocessed images are then provided to the reconstruction routine. The results of the preprocessing is demonstrated in the reconstruction of a Ti6Al4V disk. Fig. 1a and b are cross sections of the results without and with image corrections. The elimination of the beam hardening artifacts is obvious in the corrected image reconstruction. Note that we must perform these corrections to achieve an absolute measurement in contrast to the relative intensity measurement used in McFarland et al. [4]. We have found this useful for implementing the postprocessing procedure described below.

3. Tomographic reconstruction postprocessing

The size of detectable defects in tomographic reconstructions is limited by the spatial resolution

and number of the initial backprojection images. For the detection of low amounts of hydrogen in small or thin objects, postprocessing procedures become necessary. The procedure chosen is to use a computer algorithm to align the reconstruction of an object being tested with a standard object. The standard object is the same as the test object in composition and shape except the standard has little or no hydrogen. More than one object can be defined in an image, and the software aligns each object separately. After alignment the standard object image is subtracted from the test object image. The result is an image which contains only the hydrogen signal plus any data noise. Any systematic errors such as reconstruction aliases should be removed. The procedure results in improved detection capability for the small hydrogen signal as well as data which can be more easily interpreted in an automated fashion.

Consider the images resulting from the tomographic reconstruction of a test object and a standard object. The objects are assumed to be vertically aligned so only one 2-D slice is postprocessed at a time. The postprocessing algorithm creates object templates, aligns the centroids of the objects, rotates the test object, generates a difference image, and reports the difference in attenuation coefficient. The first task is to determine the extent of objects in the images. Since the minimum attenuation coefficient of the object is known, cutoff value is set which is some fraction of the coefficient (usually 0.8). A template array is generated for each image by setting the value of pixels with attenuation coefficients above the cutoff to one, and the value of pixels with attenuation coefficients below the cutoff to zero. These template arrays delineate the pixels inside the objects. The test object image is then translated so that the centroid of its template is coincident with the template centroid of the standard object. Since the test object pixels are no longer at integer locations in the standard object coordinate system, the intensities are linearly weighted to the grid. After translation the test object template is updated.

Once the template centroids are coincident, the test object can be rotated to complete the alignment. For an object of unknown shape a method is necessary to define its orientation. The ellipsoid of inertia provides the required information [7]. The angle of the principal axes with respect to the coordinate axes can be matched for the test and standard objects. It is assumed that the test and standard object orientations are within $\pm 90^\circ$ since the ellipse is symmetric about its axes. Otherwise this spatial degeneracy could result in a 180° misalignment of the object orientations. This is not a problem since the objects and turntables are always started as close as possible to the same initial position. The orientation of the principal axes is found as follows. The moments and inertial product (I_x, I_y, and I_{xy}) are determined at the centroid for each object in the template images. The principal axes of inertia are found from

$$I_p = 0.5[I_x + I_y \pm [(I_x + I_y)^2 - 4(I_x I_y - I_{xy}^2)]^{1/2}]. \quad (1)$$

The angle between the principal axes and the coordinate axes is given by

$$\theta = \arctan\left(\frac{I_x - I_p}{I_{xy}}\right). \quad (2)$$

Given these object orientations the test object is rotated about its centroid to the same angle as the standard object. After rotation a new test object template, centroid, and angle are calculated. These characteristics can be used to determine the effect of the linear weighting on the test object as well as the accuracy of the alignment.

The intensity values of the standard object images are now subtracted from the intensity values of the test object image for each individual pixel. The result is the hydrogen signal plus data noise and edge spread artifacts. Edge artifacts could arise due to slight differences in the objects' shapes, linear weighting effects, etc. Since the attenuation coefficients drop off sharply at the edges, large spurious difference signals could occur. To reduce the chance for such spurious signals, the templates for the test image and the standard image are multiplied together. The difference image is then multiplied by the combined template. Pixels which are not included in both objects (test and standard) are removed from the resulting images.

With the image comparison technique, the surface signal will be preserved as much as possible. Concentration of hydrogen, solely within surface regions of less than a pixel width (0.57 mm), would limit the ability to achieve accurate detection.

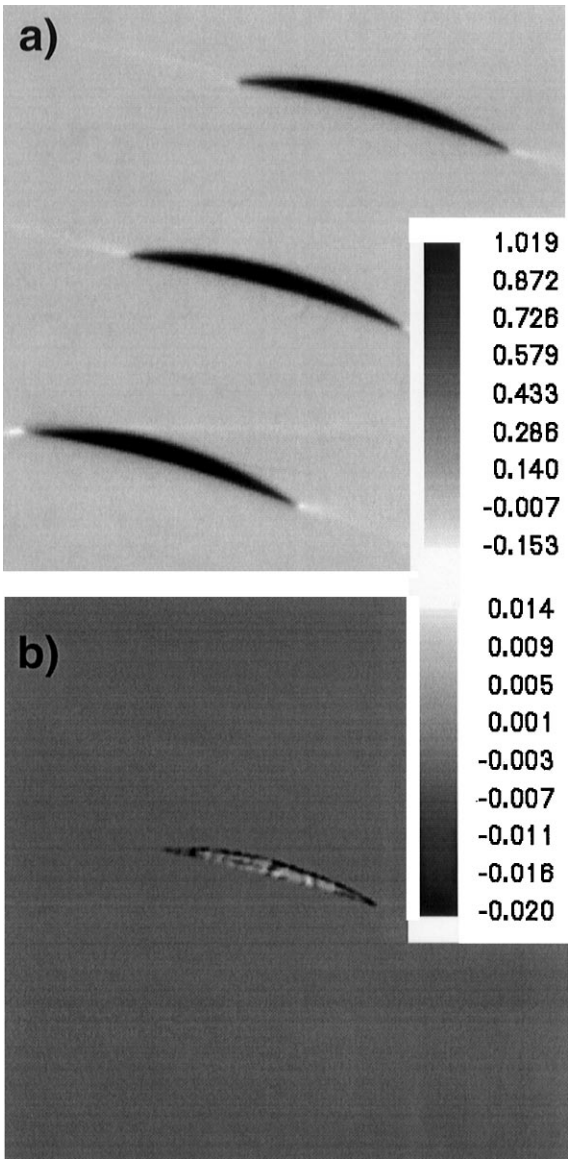

Fig. 2. Images of (a) the tomographic reconstruction with three engine compressor blades and (b) the difference in reconstructions for one of the blade positions. The scale is normalized to the attenuation coefficient of the titanium alloy.

4. Reconstruction results

The reconstruction of a set of three new compressor blades is shown in Fig. 2a. The normalized attenuation coefficient is 1.009 ± 0.008 which represents a variation of only ± 50 ppm hydrogen which is very close to that of the alloy standard of Fig. 1. In Fig. 2b the difference image generated by the alignment algorithm for one of the blades is shown. Here new blades were compared to new blades to ensure that the algorithm did not induce large spurious signals where none should exist. The alignment of objects caused a loss of approximately 3% of the pixels in the templates of the test objects. The average signal found in the difference images was equivalent to 33 ppm H with a standard deviation of 70 ppm. The signals are due to small differences in the physical size of the blades, system noise, and some residual hydrogen. We can conclude that the algorithm adequately aligns the blades and has sufficient sensitivity (noise below 200 ppm H) to report low hydrogen concentrations in images where three blades are present.

Ongoing experiments are comparing samples loaded with a calibrated amounts of H to standards with minimal H. As an example, a NIST standard of Ti6Al4V was loaded with hydrogen and calibrated with gas fusion and Cold Neutron Prompt Gamma Activation Analysis (CNPGAA) [8]. The gas pressure measurement indicated 815 ppm H and the CNPGAA indicated 827 ppm H. The density of hydrogen found with the alignment method was 844 ± 137 ppm H. The alignment of objects caused a loss of 1% of the pixels in the test object. The fluctuations are probably due to a combination of hydrogen density variation, image noise, and reconstruction aliases.

5. Conclusion

The tomography system has demonstrated the capability to detect hydrogen in titanium components to levels below 200 ppm weight with an acquisition time of 60 min. This is accomplished by correction of the backprojection images before reconstruction and comparison of standard and test objects after reconstruction.

Acknowledgements

The authors thank R.L. Paul, R.M. Lindstrom, and M. Arif for the CNPGAA results. This work was supported by the U.S. Air Force and by the U.S. Department of Energy, Lawrence Livermore National Laboratory under contract number W-7405-ENG 48.

References

[1] N.E. Patton, J.C. Williams, Hydrogen in Metals, American Society for Metals, Metals Park, OH, 1974, pp. 409–432.
[2] M.R. Gibbons, W.J. Richards, K. Shields, IEEE Trans. Nucl. Sci. (1998), submitted.
[3] E.W. McFarland, R.C. Lanza, G.W. Poulos, IEEE Trans. Nucl. Sci. 38 (1991) 612.
[4] E.W. McFarland, J. Leigh, R.C. Lanza, J. Adv. Mater. 26 (3) (1995) 3.
[5] R.H. Heusman, G.T. Gullberg, W.L. Greenberg, T.F. Budinger, Lawrence Berkeley Laboratory, CA, Pub. 214, 1977.
[6] Y. Ikeda, M. Yokoi, M. Oda, M. Tamaki, G. Matsumoto, Nucl. Instr. and Meth. A 377 (1996) 85.
[7] H. Goldstein, Classical Mechanics, Addison-Wesley, Reading, MA, 1981, pp. 198–203.
[8] R.L. Paul, M. Privett, R.M. Lindstrom, W.J. Richards, R.R. Greenberg, Metall. Mater. Trans. A 27 (1996) 3682.